# Evolutionary convergence and trophic diversity in hot vent and cold seep shrimps showcase a continuum of symbiosis

**Author & Affiliations**

Pierre Methou[1], Margaux Mathieu-Resuge[1], Loïc N. Michel[2], Valérie Cueff-Gauchard[1], Hiromi Kayama Watanabe[3], Emily J. Cowell[4], Jonathan T. Copley[5], Roxanne Beinart[6], Magali Zbinden[7], Florence Pradillon[1], Marie-Anne Cambon[1], Chong Chen[3]

[1]Univ Brest, Ifremer, BEEP, F-29280 Plouzané, France

[2]Animal Systematics and Diversity, Freshwater, and Oceanic Sciences Unit of reSearch (FOCUS), University of Liège, Liège, Belgium

[3]X-STAR, Japan Agency for Marine-Earth Science and Technology (JAMSTEC), 2-15 Natsushima-cho, Yokosuka, Kanagawa 237-0061, Japan

[4]Department of Biology, Temple University, Philadelphia, PA, USA

[5]Ocean and Earth Science, University of Southampton, Southampton, United Kingdom

[6]Graduate School of Oceanography, University of Rhode Island, Narragansett, RI, USA

[7]Laboratoire de Biologie des Organismes et Ecosystèmes Aquatiques (BOREA), MNHN, CNRS-8067, IRD-207, Sorbonne Université, UCN, UA, France, 75005 Paris, France

## Abstract

Convergent evolution offers a powerful lens through which to examine the selective forces shaping life in extreme environments. In deep-sea hot vents and cold seeps, invertebrates have independently evolved symbioses with chemosynthetic bacteria, but repeated origins of such associations within a family remain rare. Here, we investigate the evolutionary emergence of chemosymbiosis in the shrimp family Alvinocarididae across 22 species collected globally. Electron microscopy identified a gradient of epibiotic bacterial colonization within the cephalothoracic cavity, ranging from absent to dense filamentous mats, suggesting distinct trophic strategies. Isotope and lipid trophic markers confirmed difference in reliance on chemosynthetic production among sympatric species with different bacterial colonization from a single vent. Phylogenetic analysis reveals at least two independent origins of chemosymbiosis, suggesting evolutionary convergence. Microhabitat association data further show that symbiotic phenotypes are most common in shrimps occupying the hottest, most geofluid-enriched microhabitats, though exceptions suggest contributions from additional ecological or physiological constraints. Our findings reveal many alvinocaridids as gradually evolving towards symbiosis, highlighting the importance of intermediate cases to understand the pathways to chemosymbiosis. This study contributes to a broader understanding of the predictability of evolutionary outcomes in distinct habitats such as vents, with broader implications for resilience of deep-sea ecosystems.

## Introduction

Repeated evolution of similar phenotypic traits within distinct lineages is often considered as the most compelling evidence for the action of natural selection [1,2]. The recurrence of similar adaptive solutions in response to comparable environmental contexts is unlikely to arise by chance alone [3,4]. This can result from parallel evolution towards a new phenotype if ancestral phenotypes are similar, or from convergent evolution when the ancestral phenotypes are distinct [4]. While evolutionary constraints can limit phenotypic variation, the repeated emergence of analogous traits act like replicated experiments of natural selection and shed light on the underlying factors and mechanisms that govern the adaptation of species [3].

At hydrothermal vents and other deep-sea chemosynthetic ecosystems such as hydrocarbon seeps, many invertebrate species have independently evolved a symbiotic partnership with chemosynthetic bacteria as an adaption to the particular conditions of these environments [5]. In the absence of sunlight, these associations result in 'holobiont' organisms where the host is dependent on the primary production of their microbial partners, which make use of chemical energy generated by geochemical gradients in the mixing zone where seawater collides with geofluids [6]. However, not all species there are symbiotrophic – several other feeding strategies such as bacterial grazing, deposit feeding, suspension feeding, scavenging and/or predation have been reported in other species endemic to chemosynthetic environments [7–9]. For most families with symbiotrophic members, the appearance of symbiosis is a unique event either at the common ancestor of the family such as siboglinid tubeworms, mussels in the subfamily Bathymodiolinae, paskentanid snails in the sister genera *Alviniconcha* and *Ifremeria* and yeti crabs in the family Kiwaidae [5,10–12], or in a single member of a family such as the squat lobster *Shinkaia crosnieri* within Munidopsidae [13]. A notable exception are peltospirid snails, in which chemosynthetic symbioses seem to have appeared at least twice, in two distantly related genera *Chrysomallon* and *Gigantopelta* [14], and potentially even a third case in *Peltospira gargantua* [15]. In the evolutionary history of these families, the acquisition of a chemosynthetic symbiosis is not necessarily concomitant with colonization of a chemosynthetic-based habitat, questioning the respective role of selective pressures from the environment, evolutionary constraints of these hosts, and historical contingencies in the making of such symbiotic relationships.

As with peltospirid snails, alvinocaridid shrimps likely acquired chemosymbiosis several times independently, once in the sister species pair *Rimicaris exoculata*/*R. kairei* and another in the species complex *R. chacei*/*R. hybisae* [16]. These shrimps host dense communities of filamentous bacteria in their cephalothoracic cavities and on the surface of their mouthparts that harbour a great metabolic versatility, adapted to different geochemical contexts depending on the hydrothermal fields they occupy [17–19]. Three of these shrimp species (*R. exoculata*, *R. hybisae* and *R. kairei*) display a hypertrophy of their symbiont-hosting surfaces, with an inflated cephalothoracic chamber and enlarged mouthparts [16], and are considered to have a nutrition based mainly on their symbionts [20,21] with a direct nutritional transfer demonstrated for *R. exoculata* [22]. These symbiont-hosting shrimps gather in dense swarms of thousands of individuals near the vent fluid orifices, often constituting the most dominant fauna there [23,24]. Conversely, several other species in the family or even genus such as *Nautilocaris saintlaurentae, Rimicaris acuminata*, and *Rimicaris variabilis* show limited colonisation by chemosymbiotic bacteria [25]. These species tend to feed on other food sources available such as bacterial mats and/or detritus [25–28]. In *R. chacei*, the presence of a dense

bacterial colonization is not accompanied with the enlargement of cephalothorax, but results from isotopic and anatomical analyses indicate it partially depends on symbionts for nutrition in a mixed diet, while using other food sources [21,26,29]. This suggests that chemosymbiosis might be more widespread in alvinocaridid shrimps than previously identified simply by external morphology. Yet, the observation of bacterial colonization patterns remained limited to a few species and we still lack an overview of chemosymbiotic associations and diets in this family.

Our study aims to reconstruct the evolutionary history of chemosymbiosis in alvinocaridid shrimps and link it to the habitat they occupy. We address the following questions: 1) What are the patterns of bacterial colonization in different alvinocaridid species and how many time have dense bacterial colonization appeared? 2) Does alvinocaridid species with distinct colonization degrees exhibit different trophic strategies? 3) Is dense colonization by epibiotic filamentous bacteria linked to specific microhabitat occupancy along the environmental gradient of geofluid emissions in the local environment?

## Materials and Methods

### Sample collection

A total of 22 alvinocaridid shrimp species were gathered from samples originating from 32 different vent and seep localities around the globe (Table S1), collected during 31 different oceanographic expeditions between 2004 and 2023. They were mostly collected using suction samplers on either remotely operated vehicles (ROVs) or human-occupied vehicles (HOVs) and supplemented by samples from baited traps or epibenthic sledges (see Table S2 and S3 for detailed information). For scanning electron microscopy (SEM) observations, shrimp specimens were preserved either in 80% ethanol, frozen whole at -80°C, or fixed for 16h in 2.5% glutaraldehyde / filtered seawater solution, rinsed, and then preserved in filtered seawater solution at 4°C on-board of the ship. For specimens frozen whole on-board, post-fixation in 2.5% glutaraldehyde was done in the laboratory before SEM analyses. DNA extractions were carried out using individuals preserved in 80% ethanol or frozen at -80°C. Additional specimens collected at the Puy des Folles vent field on the Mid-Atlantic Ridge (MAR) during the BICOSE 3 expedition were stored frozen at -80°C for stable isotopes and lipid analyses (Table S4 and S5).

### Stable isotope and lipid analysis

The Puy des Folles hydrothermal site was selected to investigate stable isotope and fatty acid profiles of alvinocaridids because it offered the widest range of species showing distinct bacterial colonization patterns available to us, with four different species within a single hydrothermal vent locality including *Rimicaris exoculata*, *R. chacei, Mirocaris fortunata,* and *Alvinocaris markensis*. For stable isotopes analyses, pieces of abdominal muscle and mouthparts (scaphognathites – i.e., exopodite of the second maxilla – and exopodites of the first maxillipeds, hereafter called just exopodites)from three specimens per species were isolated, freeze dried and homogenized with a manual potter. Homogenized pieces of abdominal muscles from the same individuals were also used for fatty acid analyses.

Measurements of stable isotope ratio were performed by continuous flow–elemental analysis isotope ratio mass spectrometry (CF-EA-IRMS) at University of Liège (Belgium), using a vario MICRO cube C-N-S elemental analyser (Elementar Analysensysteme GMBH, Hanau, Germany) coupled to an IsoPrime100 isotope ratio mass spectrometer (Isoprime, Cheadle, United Kingdom). Isotopic ratios were expressed in ‰ using the widespread δ notation [30] relative to the international references: Vienna Pee Dee Belemnite (for carbon), atmospheric air (for nitrogen) and Vienna Canyon Diablo Troilite (for sulphur). IAEA (International Atomic Energy Agency, Vienna, Austria) certified reference materials sucrose (IAEA-C-6; $\delta^{13}C$ = -10.8 ± 0.5‰; mean ± SD), ammonium sulphate (IAEA-N-2; $\delta^{15}N$ = 20.41 ± 0.12‰; mean ± SD), and barium sulphate (IAEA-SO5, $\delta^{34}S$ = 0.5 ± 0.2‰) were used as primary analytical standards. Sulfanilic acid (Sigma-Aldrich; $\delta^{13}C$ = -25.6 ± 0.4‰; $\delta^{15}N$ = -0.13 ± 0.4‰; $\delta^{34}S$ = 5.9 ± 0.5‰; means ± SD) was used as a secondary analytical standard. Standard deviations on multi-batch replicate measurements of secondary and internal lab standards (seabass muscle) interspersed with samples (one replicate of each standard every 15 analyses) were 0.2‰ for $\delta^{13}C$, 0.1‰ for δ15N and 0.3‰ for $\delta^{34}S$. $\Delta^{13}C$ was defined as the $\delta^{13}C$ isotopic ratio of abdominal muscle tissue (the "consumer") from which was subtracted the $\delta^{13}C$ isotopic ratio of mouthparts more or less colonized by symbiotic bacteria (the "nutrition source") depending on the shrimp species. Following the same principle, $\Delta^{15}N$ and $\Delta^{34}S$ were calculated for each individual as follows: $\Delta^{15}N = \delta^{15}N_{muscle} - \delta^{15}N_{mouthpart}$ and $\Delta^{34}S = \delta^{34}S_{muscle} - \delta^{34}S_{mouthpart}$.

A minimum of 2 mg of abdominal tissue (n = 3 per species) powder were placed in pre-combusted glass vials and 6 ml of solvent mixture (CHCl3: MeOH, 2:1, v:v) were added to extract lipids. Lipid extracts were then flushed under nitrogen, sonicated, vortexed, and rested at -20°C for 24h. As described in a previous study [31], an aliquot of total lipid extract was used for transesterification. Briefly, after adding C23:0 as internal standard (free fatty acid form), lipids were first transesterified with 1ml KOH-MeOH and then with 1.6ml of $H_2SO_4$-MeOH, to form fatty acid methyl ester (FAME) that were then rinsed with distilled water saturated in hexane, and recovered within 0.4ml of hexane. FAME were analyzed on a TRACE 1300 gas chromatograph (Thermo Scientific) programmed in temperature and equipped with a splitless injector, a ZB-WAX column (30m×0.25mm IDx0.2µm) and a flame-ionisation detector, using hydrogen as vector gas. Obtained chromatograms were processed with Chromelon 7.2 (Thermo Scientific). Sixty-four FAME were identified by comparing their retention time with references from commercial mixtures (37 components FAME, PUFA1 and PUFA3, Sigma) and from house-made standards GC-MS certified; as well as by checking certain samples using mass spectrometry (GC-MS TRACE 1300 coupled to an ISQ 7000 mass spectrometer, equipped with the same apolar column and using the same program as GC-FID). Quantification of FAME in µg was based on the internal standard recovery, and then expressed in mg $g^{-1}$ of dry weight. Fatty acids relative proportions were expressed as mass percentages (%) of the total identified fatty acids.

All statistical analyses with Kruskal-Wallis and Wilcoxon tests were performed in a R v. 4.4.1 statistical environment [32].

## Scanning electron microscopy

SEM observations were carried out on 17 alvinocaridid species sampled to investigate the bacterial colonization on the cephalothoracic cavity. 48 dissected branchiostegites (inner side of the cephalothoracic cavity) and mouthparts (scaphognathites and exopodites) of individuals fixed in 2.5% glutaraldehyde were dehydrated with an ethanol series from 50% to 100% ethanol by 10%

162 increments or directly into 100% ethanol for individuals preserved in 80% ethanol. Samples were
163 then dehydrated for 5 h in a critical point dryer CPD 020 (Balzers Union, Balzers, Liechtenstein) and
164 gold-coated with a SCD 040 sputter-coater (Balzers Union). Observations and imaging were
165 performed using a Quanta 200 SEM (FEI-Thermo Fisher, Hillsboro, OR, USA).

166 We defined a colonization score for consistency when comparing our multiple SEM
167 observations. Branchiostegites (Br) were divided in three equivalent areas (anterior, center and
168 posterior) and mouthparts (Mp) in three features: the central surface, the marginal setae on the
169 edge of the mouthparts, and the additional bacteriophore setae covering the surface, present only in
170 some species (Figure S1). For each area/feature, a score from 0 to 4 was attributed according to the
171 following criteria, 0: no visible bacterial colonization; 1: a single layer of rod-shaped bacterial mats; 2:
172 colonization by rod-shaped bacteria and sparsely distributed filamentous bacteria; 3: localized spots
173 colonized by filamentous bacteria; 4: extremely dense colonization by filamentous bacteria, the
174 surface of shrimp cuticle barely visible. The final colonization score is obtained by the addition of
175 each areas/features colonization scores for a total score of 0 to 24. We reanalysed the SEM dataset
176 from a previous study [25] to define the colonization scores of species analyzed by this study (*R.*
177 *variabilis*, *R. acuminata* and *N. saintlaurentae*). We based our colonization scores of *R. exoculata* and
178 *R. kairei* from descriptions of their cephalothoracic symbioses in the literature [17,19].

179 **DNA extraction and sequencing**

180 We performed DNA extractions on individuals from the same 22 alvinocaridid species
181 sampled using pieces of abdominal tissues or the 4th/5th pleopods with the DNeasy Blood & Tissue
182 kit (Qiagen, Hilden, Germany) following the manufacturer's instructions. Partial fragments of the
183 nuclear 18S rRNA (905 bp), and the mitochondrial 16S rRNA (515 bp) and the cytochrome oxidase *c*
184 subunit I (COI) gene (743 bp) were amplified respectively with the 18S-1f & 18S-5r, the Cari16S-1F
185 and Cari16S-1R [33], and the CariCOI-1F and CariCOI-1R primers [21]. We used ExTaq polymerase
186 (Takara) or GoTaq polymerase (Promega) in 25µl reactions for PCR amplifications with the following
187 cycling conditions: 40 cycles at 51°C as the annealing temperature for 18S, 35 cycles at 55°C for 16S,
188 and 35 cycles at 50°C for COI. Bi-directional Sanger sequencing was conducted by Eurofins (Köln,
189 Germany) or by the FASMAC Corporation (Kanagawa, Japan) for the different PCR products. We used
190 Geneious Prime® 2023.1.2 (https://www.geneious.com) to edit and align sequence chromatograms.
191 We carried out phylogenetic reconstruction using the Mr Bayes plugin v3.2.6 [34] in Geneious.
192 Bayesian inference was run with the GTR + G + I substitution model and 1 million MCM steps,
193 discarding the first 10 000 steps and with a subsampling frequency of 4000 steps. Best fitting model
194 was selected with Modeltest [35] within Geneious. Ancestral state reconstruction was conducted
195 with the ace function of the phytools v2.4-4 package [36] in RStudio v4.4.1.

196

197 **Results**

198 **Stable isotope and lipid analysis**

199 Within a single hydrothermal vent field - Puy des Folles on the Mid Atlantic Ridge - each of
200 the four alvinocaridid species displayed clearly distinct fatty acid and stable isotope composition
201 (Figure 1). The $\delta^{15}N$ of most alvinocaridid mouthparts was significantly lower than the $\delta^{15}N$ of
202 abdominal muscles from the same species (Wilcoxon test; W= 118, p-value < 0.01), except for *A.*

*markensis* that showed the opposite trend with equivalent or higher $\delta^{15}N$ values of mouthparts compared to abdominal muscles. Inter-specific differences in nitrogen trophic shift ($\Delta^{15}N$) were present (Kruskal–Wallis; $\chi^2 = 9.46$, p-value < 0.05), with higher values for the two *Rimicaris* species (*R. exoculata*: $\Delta^{15}N = 3.17 \pm 0.17$; *R. chacei*: $\Delta^{15}N = 3.34 \pm 0.95$) compared to *A. markensis* ($\Delta^{15}N = - 0.05 \pm 1.53$). The $\delta^{13}C$ did not vary between muscles and mouthparts (Wilcoxon test; W= 90, p-value > 0.05), but varied among species (Kruskal–Wallis; $\chi^2 = 17.79$, p-value < 0.001) with a significant $^{13}C$-enrichment for *R. exoculata* and *M. fortunata* compared to *R. chacei* and *A. markensis*. Carbon trophic shift ($\Delta^{13}C$) was high in *R. chacei* compared to other alvinocaridids, which exhibited low $\Delta^{13}C$ values in *R. exoculata* and *M. fortunata* or even negative values for *A. markensis*. As for carbon, $\delta^{34}S$ did not vary between tissues (Wilcoxon test; W= 57, p-value > 0.05) but varied among species (Kruskal–Wallis; $\chi^2 = 15.9$, p-value < 0.001) with a significant $^{34}S$-depletion for *M. fortunata* and *A. markensis* compared to the two *Rimicaris* species (Figure S2).

Overall, species differed in their total fatty acid content (Kruskal–Wallis test, H25 = 9.67, p-value < 0.05; Table S5). *Rimicaris* species had the higher significant total contents with 207.0 ± 34.0 and 181.0 ± 27.0 mg $g^{-1}$ for *R. exoculata* and *R. chacei*, respectively. *M. fortunata* (24.7 ± 2.4 mg $g^{-1}$) and *A. markensis* (20.8 ± 0.9 mg $g^{-1}$) contained fatty acid contents 10 and 8.3 times lower than *R. exoculata*, respectively. The fatty acid compositions of shrimp abdominal muscles varied significantly among species (PERMANOVA, df = 3, F = 5.34, $r^2 = 0.59$, p-value < 0.001), as highlighted by the PCA on which the two first axis explained 48% of the total inertia (26.76 % on the first axis and 22.17 % on the second, Figure 1A). The fatty acids profiles of the two *Rimicaris* species were positively related to axis 2, while that the two other species were negatively related to this axis. Individuals of *R. exoculata* and two of *R. chacei* were characterized by high proportions of short chain fatty acids mainly composed of 14:0, 14:1n-7, 16:1n-5, 16:2n-4, 18:2n-4, 18:3n-4, 18:2n-7 and by the 20:3nmi (non-methylene interrupted) (Figure 1A). Individuals of *A. markensis* and one of *R. chacei* were discriminated positively on the first principal axis and characterized by higher proportions of longer chain fatty acids, such as 20:4n-6, 20:5n-3, 22:5n-3, 22:6n-3 and the 18:1n-9DMA (dimethylacetal) (Figure 1A). Individuals of *M. fortunata* were negatively discriminated on the first and second principal axis, and characterized by higher proportions of monounsaturated fatty acids, such as 16:1n-7, 18:1n-7, 18:1n-9, 22:1n-7 and the 20:2nmi (Figure 1A).

## SEM observations

For most of the 22 alvinocaridid species observed, some general trends of bacterial colonization on branchiostegites and on mouthparts emerge (Figure 2 and Table S2). Overall, branchiostegites were generally devoid of colonization with only a few spots of rod-shaped bacteria in a single layer or a few scattered filamentous bacteria, most often on the anterior one-third (Figure 2; exemplified by *R. leurokolos* and *M. fortunata*). Mouthparts – scaphognathites and exopodites – show similar colonization patterns on most of their surfaces but contrast by a denser colonization on the plumose setae structures aligned along their margins (Figure 2; exemplified by *R. leurokolos* and *M. fortunata*). This results in total colonization scores between 3 and 10 score for most alvinocaridid species.

Apart from these general trends, some species show more specific colonization patterns (Figure 2 and Table S1). Among them, *Rimicaris hybisae* and *R. chacei* differ drastically from the other species by a very dense colonization of filamentous bacteria on all structures except on the posterior part of the branchiostegite. These two species were mainly distinguished by a more advanced

colonization of dense filamentous bacteria covering the anterior two-thirds of the branchiostegite for *R. hybisae* (Figure 2) and the anterior one-third only for *R. chacei*. These two species also show additional bacteriophore setae structures (less numerous in *R. chacei*) on the entire mouthpart surfaces offering additional colonisation areas compared to other alvinocaridids, further enhancing their colonization score (*R. hybisae*: 22; *R. chacei*: 18 to 20). Based on the literature, a similarly dense colonization of filamentous bacteria on all structures except on the posterior third of the branchiostegite with a colonization score of 22 can be attributed to *R. kairei* and *R. exoculata* [17,19].

Two other *Rimicaris* species – *R. vandoverae* and *R. cambonae* – also departs from the general pattern with a dense colonization by filamentous bacteria on the anterior one-third of their branchiostegite (Figure 2), and to some extent, on their mouthpart surfaces as well, leading to total colonization scores of 12 to 13 for *R. vandoverae* and of 11 to 13 for *R. cambonae*. In addition, two *Alvinocaris* species – *A. lusca* and *A. costaricensis* – consistently exhibit dense spots of filamentous bacteria, not only on the marginal setae but also on the surfaces of their mouthparts in all individuals observed (Figure 2), as well as on the anterior one-third of the branchiostegites in some individuals (*A. lusca* scores: 11 to 12; *A. costaricensis* scores: 9 to 12). Finally, in contrast to all other species, *A. markensis* shows a nearly complete absence of bacterial colonization on all of these structures (Figure 2), even on marginal setae of their mouthparts which were typically colonized in all other species (Figure 2), leading to a score of 0 or 1.

## Phylogenetic and Ancestral state reconstruction

Our phylogenetic reconstruction of Alvinocarididae based on multi-gene alignment (*COI*, *16S* and *18S*) using Bayesian inference (Figure 2) recovered a strongly supported monophyly of the family (Bayesian Posterior Probability (BPP) = 1) as well as the monophyly of the genera *Rimicaris* (BPP = 0.99) and *Alvinocaris* (BPP = 0.89). The clade formed by *Mirocaris fortunata* + *Nautilocaris saintlaurentae* was the early-diverging lineage, sister to all the other alvinocaridid shrimps. All nodes were well-supported (BBP > 0.8), except one node within *Rimicaris* (BPP = 0.77). Ancestral state reconstruction supported two distinct origins for the appearance of a symbiotic phenotype: once at the common ancestor of *R. exoculata* and *R. kairei* and once in the *R. chacei*/*R. hybisae* species complex (Figure 2). It also supported multiple origins for the appearance of mixed or potentially mixed phenotypes (Figure 2). Ancestral state reconstruction of habitats revealed that a vent origin was most likely for the most recent common ancestor of Alvinocarididae with a secondary colonisation of hydrocarbon seeps in *A. costaricensis* and in the common ancestor of one of the two major clades within genus *Alvinocaris* clade (Figure S3).

## Habitat and colonization score

The relationship between the colonization score of an individual and its type of habitat was not entirely straightforward (Figure 3). All species with high colonization scores – i.e., score > 18 – such as the *R. exoculata*, *R. kairei*, *R. hybisae/R. chacei* complex – were always found in close proximity to vent fluid emissions. However, not all alvinocaridid species occupying similar habitat, such as *R. leurokolos* or some individuals of *R. variabilis*, necessarily showed such high colonization scores (Figure 3). Indeed, *R. leurokolos* shrimps showed more similar colonization scores to *A. longirostris* or *A. dissimilis* individuals from the same site but inhabiting cooler habitats within mussel beds or near *Shinkaia* aggregates. In addition, species with mid-range colonization score – i.e., score >10 – like *R. vandoverae*, *R. cambonae*, or *A. lusca* were found to inhabits cooler habitats than

288 chimney surfaces such as *Alviniconcha* snail colonies or even cooler ones such as mussel beds.
289 *Alvinocaris markensis* which displayed lowest colonization score were always found in peripheral
290 areas away from the venting fluid.

291

## 292 Discussion

293 This study shows the presence of distinct trophic strategies among species of alvinocaridid
294 shrimps that display different degrees of bacterial colonization within the same locality, as supported
295 by our stable isotope and fatty acid analyses (Figure 1 & S1). As indicated by previous studies, the
296 nutrition of *Rimicaris exoculata* is mainly based on its bacterial ectosymbionts [17,21,22]. Here, we
297 recorded important values for $\Delta^{15}N$ between the host organs (i.e., mouthparts) and muscle tissues of
298 this species. This is generally expected between a consumer and its food items, which consistent with
299 ectosymbionts being a major food source for this species. This is further supported by a fatty acid
300 composition enriched in 16:2n-4 and 18:2n-4 sulfuric oxidative filamentous bacterial markers [37].
301 On the other end of the spectrum, *Alvinocaris markensis* showed a near absence of colonization,
302 which is consistent with a non-symbiotic nutrition. The isotopic composition of its mouthparts and
303 muscles were similar (absence of marked trophic shift), which is expected for two tissues synthesized
304 independently by the same animal and does not suggest any trophic relationship. Their fatty acid
305 compositions were also enriched in omega-3 and -6 long chain polyunsaturated fatty acids, which can
306 be either associated to the ingestion of phytodetritus [37] and/or biosynthesised by bacteria [38,39].
307 In the same way, the limited bacterial colonization observed in *M. fortunata* is in line with limited
308 inputs from its symbionts, demonstrated by a lower trophic shift and a distinct monounsaturated
309 fatty acid composition often associated to thio-oxidizing bacteria [40]. Our trophic marker data on *R.*
310 *chacei* individuals are also consistent with previous works suggesting a mixotrophic diet for this
311 species [21,29].

312 Taken together, our results illustrate niche theory predicting that sympatric species are
313 partitioned in their feeding habits and resource use to avoid competitive exclusion among the four
314 studied species [41]. Through their symbiotic associations, host species such as *Rimicaris* are likely to
315 access novel niches that are expanded by the addition of symbiont's physiological and metabolic
316 capacities [5]. A partnership with symbionts likely guarantees access to larger and more consistent
317 quantities of food, as highlighted by the higher total fatty acid contents found in these two species.
318 In chemosynthesis-based ecosystems, niche partitioning in relation to symbioses have been
319 demonstrated in *Alviniconcha* snails where different hosts harbour variable symbiont phylotypes
320 within the same region [42]. In alvinocaridid shrimps, the partitioning among sympatric species
321 seems to be driven by various degrees of reliance on the production of their filamentous bacterial
322 symbionts, from none to full dependence.

323 By expanding our assessment of bacterial colonization patterns to a global dataset of 22
324 alvinocaridid species, we revealed the presence of a gradient of colonization phenotypes within the
325 family, with lineages associated with symbiotrophic, mixotrophic (or potentially mixotrophic) diets.
326 This suggests an evolutionary convergence with multiple emergences of symbiotic phenotypes along
327 the evolutionary history of Alvinocarididae (Figure 2), implying that this group has high flexibility in
328 the development of distinct trophic strategies. Although uncommon in other chemosymbiotic
329 holobionts, nutritional flexibility with limited contribution from heterotrophy has also been shown in

330 several bathymodioline mussels which retain some ability to filter-feed [43,44], or *Alviniconcha* snails
331 which can still digest some food with their reduced gut [45]. In alvinocaridid shrimps, this trophic
332 flexibility can be further extended when considering the case of the *R. chacei*/*R. hybisae* species
333 complex that display a developmental plasticity during their metamorphosis in the colonization
334 surfaces of their symbiont-hosting organs, allowing individuals to perform either mixotrophic or
335 symbiotrophic feeding depending on the environment [16]. This developmental variability could be
336 due to competitive interactions for niche occupancy with *R. exoculata* at juvenile stages promoting a
337 shift toward mixotrophy on MAR vents [24], while *R. hybisae* in the Mid-Cayman Spreading Centre
338 has no local competitor and can fully develop its symbiotrophic phenotypes [23]. We suggest that
339 other cases of niche partitioning are driving feeding strategies and symbiont colonization in
340 alvinocaridids such as between *A. marimonte*, *R. cambonae*, and *R. loihi* living in sympatry on the
341 Mariana Arc [27,46].

342 Our analyses also support habitat specialization as a key factor shaping symbiotic relationships in
343 alvinocaridid shrimps (Figure 3). At an ecosystem-scale, the acquisition of sulfur-oxidizing or
344 methanotrophic symbionts in bathymodioline mussels and vesicomyid clams coincides with their
345 repeated colonisations in different types of chemosynthetic habitats along their evolutionary
346 histories [11,47]. Similarly, the origin of chemosymbiosis in the abyssochrysoidean snails coincide
347 with the Aptian oceanic anoxic event which allowed them to colonize hydrothermal vents, though
348 the other major clade that split at the same time, containing genera such as *Provanna* and
349 *Desbruyeresia*, did not evolve symbiosis [48]. Symbiosis in 'vestimentiferan' worms in the family
350 Siboglinidae also evolved only once at the start of their association with reducing habitats, but its
351 origin traces back widespread reducing, anoxic sediments instead of sparse and ephemeral vents or
352 seeps [49]. These scenarios contrast with the emergence of chemosynthetic symbiosis in
353 alvinocaridid shrimps, which is not directly linked to their colonization of reducing habitats, as our
354 ancient habitat reconstruction indicated that association with hydrothermal vents is ancestral to the
355 family. Instead, the symbiosis appeared secondarily, more similar to the case of some peltospirid
356 snails [14,15]. Yet, at the microhabitat scale, the habitat preference of alvinocaridid species along the
357 geochemical gradient appears to be important, as all species with high colonization scores occupy
358 the hottest parts of the vent chimney with the greatest exposure to high concentrations of geofluids.
359 This emphasizes the strong influence of the geochemical gradient in structuring the distribution and
360 zonation of chemosynthetic holobiont species [5,6]. However, this link is not always clear-cut, with
361 some alvinocaridid species of potentially mixed phenotypes inhabiting coolers habitats (e.g., *A. lusca*
362 and *R. cambonae*) and species displaying limited epibiont colonization inhabiting hot venting areas
363 (e.g., *R. leurokolos*), suggesting that other factors, including the co-occurrence with other abundant
364 holobionts, are also at play for establishment of their realized niches.

365

366 The limited number of known chemosynthetic symbioses in crustaceans compared to annelids
367 and molluscs [5,50] may be linked to evolutionary constraints of the phylum such as their moulting
368 cycle. In symbiotic insects, moulting only during the early phases of their life cycles poses a challenge
369 to the transmission and maintenance of symbiotic partnerships [51], which is further enhanced in
370 crustaceans that moult throughout their adult life. In *R. exoculata*, the moulting does not hamper the
371 establishment of a chemosynthetic symbiosis but the very rapid moulting frequency, estimated at
372 every ten days, imposes a rapid renewal rate of the symbiont community [52], probably resulting in a

373 significant metabolic cost. The high mobility of decapod crustaceans could also be another barrier to
374 the emergence of symbiotic relationship in this group. Indeed, global functional trait analyses of
375 hydrothermal vent ecosystems have highlighted that most species with a symbiotic feeding mode
376 were sessile or only slightly mobile [53]. A high motility allows species to significantly expand
377 accessible food resources instead of relying on a single trophic strategy, which could explain the
378 gradual variations of symbiont colonization phenotypes we observe among alvinocaridid species.

379 These two factors – i.e., moulting and mobility – should also be mentioned as potential sources
380 of bias in our observations which could contribute partly to the observed inter-individual variability
381 of bacterial colonization observed. For our observations, we excluded individuals just after moulting
382 – characterised by soft carapaces and a lack of mineral deposition – that have reset their epibiont
383 colonization [52]. However, we cannot rule out that different individuals observed could be at slightly
384 different moult – and thus bacterial colonization – stages. Similarly, with alvinocaridid shrimps being
385 mobile, we cannot be sure if the sampling habitat differs or not from the habitat of that individual in
386 the past few hours/days, especially for species known to occupy a wide range of habitat types such
387 as *A. longirostris*, *R. variabilis* or *R. chacei* [24,28] (see also Figure 3). However, these potential biases
388 are unlikely to affect the general trends we highlight, with several species, such as *R. leurokolos*,
389 being restricted to a single type of habitat [28,54].

390 Overall, rather than a division in two categories of symbiotic and non-symbiotic species, our
391 results indicate that chemosymbiosis gradually emerged in alvinocaridid shrimps, under the influence
392 of the geochemical gradient but not only that. Our observations highlight a more complex and
393 ongoing dynamic in the emergence of symbioses in vent and seep endemic species. As *R. chacei* and
394 other shrimps with mixotrophic diet, several species in other phyla could be partially symbiotic. To
395 some extent, mixotrophy has already been demonstrated in bathymodioline mussels. Many other
396 examples inferred from stable isotopic compositions and/or observations of bacterial ectosymbionts
397 could represent cases of partially chemosymbiotic species such as the amphipod *Exitomelita sigynae*
398 [55] or the small vent snails *Peltospira smaragdina* and *Cyathermia naticoides* [8,56]. We argue that
399 studying these gradual cases of chemosymbiosis is as essential as studies of symbioses from
400 emblematic foundational species to fully understand the evolutionary dynamics of how symbiotic
401 relationships are established.

402 Our results also have significant implications for the conservation of hydrothermal vent
403 ecosystems. A recent study [53] highlighted the high proportion of functionally unique species with
404 little redundancy in hydrothermal vents resulting in rapid collapse of these ecosystems using
405 simulated species extinction – but the feeding modes of all alvinocaridids were categorized as
406 bacterivores. Our work suggests there is more nuance with a continuum in terms of feeding modes
407 within this family. Rather than diminishing the conclusions of that study [53], we further enhance the
408 view of high functional uniqueness in vent endemic species which points again to the vulnerability of
409 these environments in the face of mining threats.

410

411 ## Conclusion

412 By investigating bacterial colonisation and trophic markers in alvinocaridid shrimps in an
413 unprecedented global-scale study of 22 species, we underscore that the evolution of chemosynthetic

symbiosis in alvinocaridid shrimps is a dynamic and recurrent process shaped by complex factors including ecological context, developmental plasticity, and phylogenetic constraints. The independent emergence of densely colonized symbiotic phenotypes, coupled with a spectrum of intermediate forms, points to evolutionary convergence driven by strong environmental selection. Yet, the incomplete correspondence between symbiosis and habitat, and the persistence of mixed trophic strategies, highlight the role of other factors like the physiological and developmental constraints due to moulting and mobility in modulating evolutionary trajectories. Our study exemplifies how complex traits such as symbiosis at vents and seeps can, and are being, evolved incrementally, through flexible and sometimes facultative intermediates, rather than through abrupt transitions as is seen in other groups like abyssochrysoid snails and vesicomyid clams. This continuum challenges simplistic categorizations of broader taxonomic groups inhabiting vents and seeps under one or a couple of feeding modes, since Alvinocarididae clearly includes a whole spectrum of feeding modes. Our work contributes to a more nuanced understanding of the repeatability — and limitations — of evolution in 'extreme' environments.

## Acknowledgments

We thank the captain, crew, and scientists on-board R/V *Pourquoi Pas?* during research expeditions BICOSE2014 (https://doi.org/10.17600/14000100), BICOSE2 (https://doi.org/10.17600/18000004), BICOSE3 (https://doi.org/10.17600/18002399), BIOBAZ (https://doi.org/10.17600/13030030), HERMINE2 (https://doi.org/10.17600/18001851), and WACS (https://doi.org/10.17600/11030010), R/V *Atalante* during expeditions CHUBACARC (https://doi.org/10.17600/18001111), FUTUNA3 (https://doi.org/10.17600/12010040), and MOMARSAT21 (https://doi.org/10.17600/18001296), R/V *Shinsei Maru* during expeditions KS-21-20 and KS-22-2, R/V *Natsushima* during expedition NT15-02, R/V *Kaimei* during expedition KM23-E05, R/V *Kaiyo* during expedition KY14-01, R/V *Yokosuka* during expeditions YK10-11, YK19-10, YK16-E02, YK22-05, YK23-06, and YK23-16, R/V *Haiyang 6* during expedition HYDZ6-2020-05, R/V *Tangaroa* during expeditions TAN0411, TAN1206, and TAN2102, R/V *Ka'imikai-o-Kanaloa* during expeditions KOK0506 and KOK0507, R/V *James Cook* during expedition JC82, R/V *Falkor (too)* during expedition FKt231024, R/V *Atlantis* during expedition AT42-03 and R/V *Thomas G. Thompson* during expedition TN401. We extend the same to the pilots and technical teams of ROVs *Victor 6000*, *Hyper-Dolphin, KM-ROV*, *Haima2*, *Isis*, *Ropos*, *SuBastian*, and *Jason II* as well as the HOVs *Nautile*, *Shinkai 6500*, *Pisces V*, and *Alvin* during those expeditions. We gratefully acknowledge the cruise PIs for leading the expeditions: François Lallier, Sorbonne Université (BIOBAZ); Didier Jollivet and Stéphane Hourdez, CNRS (CHUBACARC); Yves Fouquet (FUTUNA3); Cécile Cathalot and Ewan Pelleter, Ifremer (HERMINE2); Marjolaine Matabos and Jozée Sarrazin, Ifremer (MOMARSAT21); Karine Olu, Ifremer (WACS); Ken Takai, JAMSTEC (KY14-01, YK19-10, YK16-E02, YK22-05, KM23-E05); Masahiro Yamamoto, JAMSTEC (NT15-02, YK23-06); Shigeaki Kojima, AORI, the University of Tokyo (YK10-11); Takafumi Kasaya, JAMSTEC (NT15-02), Tatsuo Nozaki, Waseda University (KS-21-20); Hironori Komatsu, National Museum of Nature and Science (KS-22-2); Kenichiro Tani, National Museum of Nature and Science, Japan (YK23-16S); Jun Tao, Guangzhou Marine Geological Survey (HYDZ6-2020-05); Gary Massoth and Bob Embley, NOAA (KOK0505, KOK0506, KOK0507); Malcolm Clark, NIWA (TAN1206); Laura Wallace, New Zealand Institute of Geological and Nuclear Sciences (TAN2102); John W. Jamieson, Memorial University of Newfoundland (FKt231024) and Erik Cordes, Temple University (AT42-03). Biological sampling within

the Commonwealth of the Northern Mariana Islands was carried out under the Marine Scientific Research permit number MSR U2022-047 from the United States government. This is a GACHINKO cruise Episode I (YK19-10) and Episode III (YK22-05) output. We are indebted to the Kingdom of Tonga and the government of Papua New Guinea for permitting access to their national waters and resources. We obtained the agreement to sample in Wallis et Futuna waters from the Haut Commissariat à la République in New Caledonia and the Préfecture in Wallis and Futuna. We thank Kareen Schnabel (NIWA) for providing samples from the Kermadec Arc and Hikurangi Margin, Aotearoa/New Zealand, Jianwen Qiu for providing samples from methane seep of the South China Sea and Hidetaka Nomaki (JAMSTEC) for providing facilities and discussions that helped in drafting this manuscript. We also thank Nicolas Gayet (UMR BEEP; Ifremer) and Katsuyuki Uematsu (Marine Work, Japan) for their work in preparing samples for scanning electron microscopy.

## Funding

PM was supported by ISblue project, Interdisciplinary graduate school for the blue planet (ANR-17-EURE-0015) and co-funded by a grant from the French government under the program "Investissements d'Avenir" embedded in France 2030. Analyses conducted during this study also benefited from French State aid managed by the National Research Agency under France 2030 LIFEDEEPER: ANR-22-POCE-0007. This study was supported by the Cooperative Research Program of Atmosphere and Ocean Research Institute, The University of Tokyo (R/V *Yokosuka*, cruise YK23-16S). Sample collection on TN401 by EC and RAB was supported by the US National Science Foundation award OCE-1736932 to RAB. This study was also supported by Council for Science, Technology, and Innovation (CSTI), Japan as the Cross Ministerial Strategic Innovation Promotion Program (SIP), Next-generation Technology for Ocean Resource Exploration. RRS *James Cook* cruise JC82 was funded by the UK Natural Environment Research Council grant NE/F017774/1 to JTC. The FKt230303 expedition was funded by the Schmidt Ocean Institute, who also provided funding for making this paper Open Access. The AT42-03 expedition off Costa Rica was funded by the NSF grant NSF OCE 1635219.

## Figures

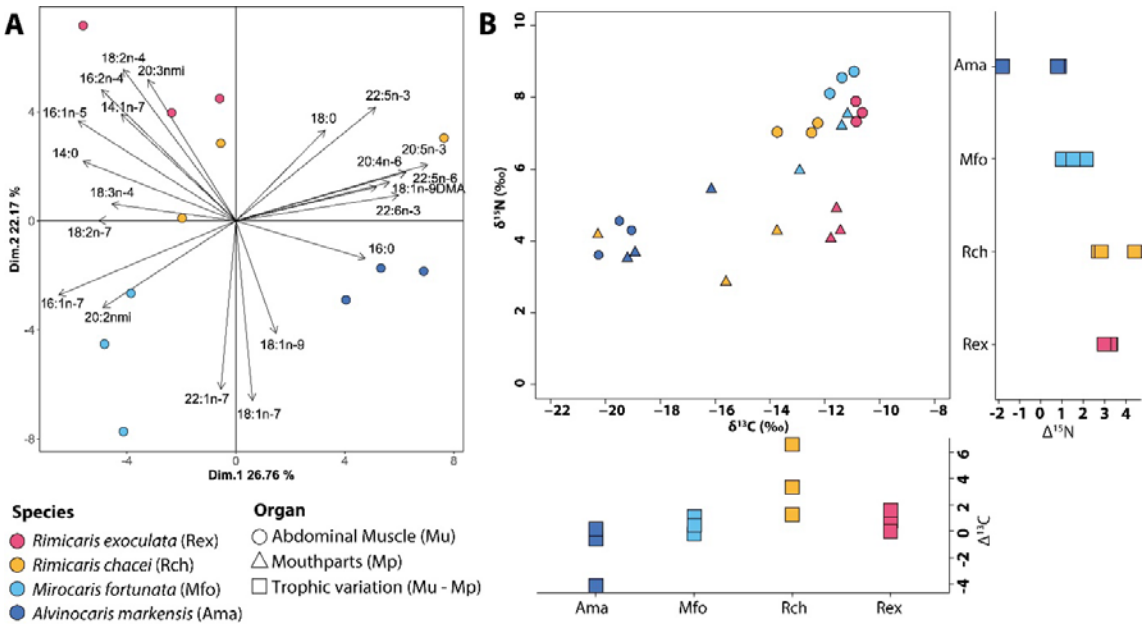


**Figure 1.** Trophic strategies of alvinocaridid species displaying different degree of bacterial colonization at the Puy des Folles vent field. Colors indicates shrimp species and shape indicates organ analyzed. **A.** Principal Component Analyses (PCA) of fatty acid composition (expressed in mass %) of the abdominal muscles from the distinct alvinocaridid species **B.** Carbon and nitrogen isotopic ratios of abdominal muscles and mouthparts from alvinocaridid shrimps. $\Delta^{13}C$ and $\Delta^{15}N$ display variations of carbon and nitrogen ratios between muscles and mouthpart tissues of each individual.

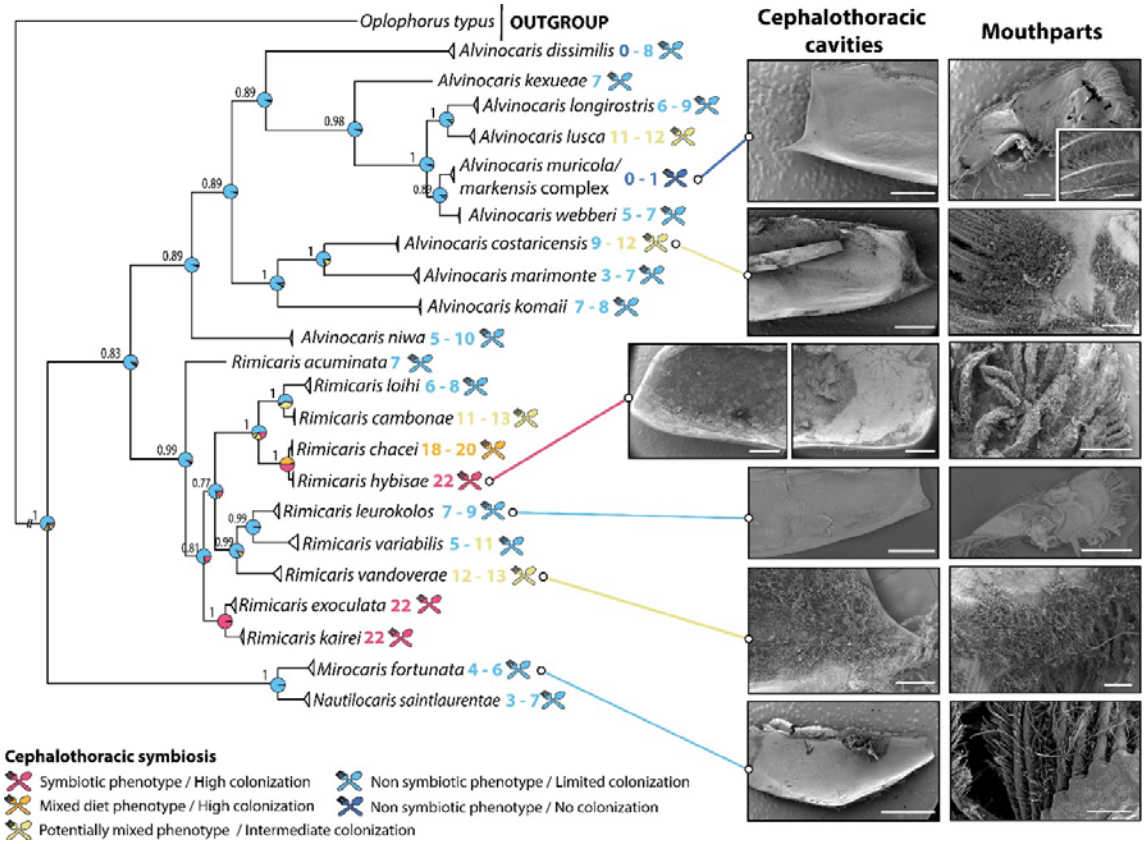


**Figure 2.** Evolutionary history of the chemosynthetic symbiosis in alvinocaridid shrimps **(left)** Phylogenetic tree of Alvinocarididae based on Bayesian inference (GTR + G + I model) generated from a 2177 bp concatenated alignment comprising partial fragments of the 18S, 16S, and COI genes. Coloured numbers associated to each species indicate the range of colonization scores defined from SEM observations and colours correspond to the different categories of chemosymbiotic phenotypes (see legend). Numbers on each node indicate Bayesian Posterior Probabilities (BPP) of the phylogeny and pie charts represent ancestral phenotypes displaying posterior probabilities of each node being in each category of phenotypes. **(right)** Representative examples of SEM observations for the cephalothoracic cavities and mouthparts linked to the alvinocaridid species observed. Scale bars from top to bottom for cephalothoracic cavities: *A. muricola* overview (1 mm); *A. costaricensis* (2 mm); *R. hybisae* (2 mm); *R. leurokolos* (1 mm); *R. vandoverae* (500 µm); *M. fortunata* (2.5 mm). Scale bars from top to bottom for mouthparts: *A. muricola* overview (1 mm) and close up (100 µm); *A. costaricensis* (250 µm); *R. hybisae* (1 mm); *R. leurokolos* (1 mm); *R. vandoverae* (250 µm); *M. fortunata* (50 µm). Additional SEM observations for all studied species are provided in Figure S4 and S5.

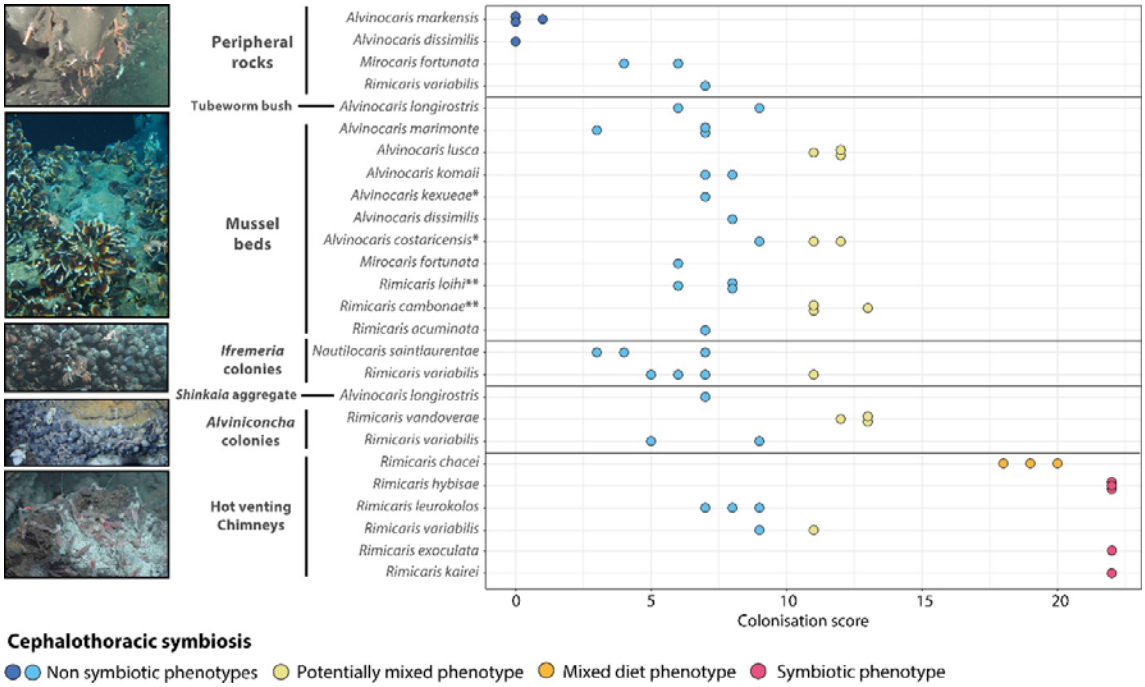


**Figure 3.** Individual colonization scores of each alvinocaridid species as a function of their habitat along the geochemical gradient. The habitats are ordered according to their distance to the venting or seepage emissions from close distance on the bottom and further away on top of the plot. Sampling of Alvinocaridids shrimps off New Zealand with an epibenthic sledge did not allow to associate a habitat type with their individual colonization scores. *: Species collected from methane seeps. **: *R. cambonae* and *R. loihi* were collected within a mussel bed in close vicinity to a hot venting habitat. These shrimps were found in both habitats [46] with individuals likely moving from one to another. Habitats types of alvinocaridid shrimps are illustrated by (from top to bottom): a peripheral rock habitat at Puy des Folles (Mid Atlantic Ridge); a mussel bed habitat at Minami-Ensei (Okinawa Trough); a *Ifremeria* snail colony at Susu Knolls (Manus Basin); an aggregation of *Alviniconcha* snails at Snail site (Mariana back-arc basin); a shrimp assemblage near hot venting fluids at PACMANUS (Manus Basin).

## References


1. Arendt J, Reznick D. 2008 Convergence and parallelism reconsidered: what have we learned about the genetics of adaptation? *Trends in Ecology & Evolution* **23**, 26–32. (doi:10.1016/j.tree.2007.09.011)

2. Losos JB. 2011 Convergence, adaptation, and constraint. *Evolution* **65**, 1827–1840. (doi:10.1111/j.1558-5646.2011.01289.x)

3. Sackton TB, Clark N. 2019 Convergent evolution in the genomics era: new insights and directions. *Phil. Trans. R. Soc. B* **374**, 20190102. (doi:10.1098/rstb.2019.0102)

4. Cerca J. 2023 Understanding natural selection and similarity: Convergent, parallel and repeated evolution. *Molecular Ecology* **32**, 5451–5462. (doi:10.1111/mec.17132)

5. Sogin EM, Kleiner M, Borowski C, Gruber-Vodicka HR, Dubilier N. 2021 Life in the Dark: Phylogenetic and Physiological Diversity of Chemosynthetic Symbioses. *Annual Review of Microbiology* **75**, 695–718. (doi:10.1146/annurev-micro-051021-123130)

6. Sogin EM, Leisch N, Dubilier N. 2020 Chemosynthetic symbioses. *Current Biology* **30**, R1137–R1142. (doi:10.1016/j.cub.2020.07.050)

7. Govenar B. 2012 Energy Transfer Through Food Webs at Hydrothermal Vents: Linking the Lithosphere to the Biosphere. *Oceanography* **25**, 246–255. (doi:10.5670/oceanog.2012.23)

8. Portail M, Brandily C, Cathalot C, Colaço A, Gélinas Y, Husson B, Sarradin PM, Sarrazin J. 2018 Food-web complexity across hydrothermal vents on the Azores triple junction. *Deep-Sea Research Part I: Oceanographic Research Papers* **131**, 101–120. (doi:10.1016/j.dsr.2017.11.010)

9. Van Audenhaege L, Fariñas-Bermejo A, Schultz T, Lee Van Dover C. 2019 An environmental baseline for food webs at deep-sea hydrothermal vents in Manus Basin (Papua New Guinea). *Deep-Sea Research Part I: Oceanographic Research Papers* **148**, 88–99. (doi:10.1016/j.dsr.2019.04.018)

10. Roterman CN, Lee W, Liu X, Lin R, Li X, Won Y. 2018 A new yeti crab phylogeny: Vent origins with indications of regional extinction in the East Pacific. *PLOS ONE* **13**, e0194696. (doi:10.1371/journal.pone.0194696.s011)

11. Lorion J, Kiel S, Faure B, Kawato M, Ho SYW, Marshall B, Tsuchida S, Miyazaki JI, Fujiwara Y. 2013 Adaptive radiation of chemosymbiotic deep-sea mussels. *Proceedings of the Royal Society B: Biological Sciences* **280**, 20131243. (doi:10.1098/rspb.2013.1243)

12. Breusing C, Genetti M, Russell SL, Corbett-Detig RB, Beinart RA. 2022 Horizontal transmission enables flexible associations with locally adapted symbiont strains in deep-sea hydrothermal vent symbioses. *Proceedings of the National Academy of Sciences* **119**, 1–11. (doi:10.1073/pnas.2115608119)

13. Watsuji T, Yamamoto A, Motoki K, Ueda K, Hada E, Takaki Y, Kawagucci S, Takai K. 2015 Molecular evidence of digestion and absorption of epibiotic bacterial community by deep-sea crab *Shinkaia crosnieri*. *The ISME Journal* **9**, 821–831. (doi:10.1038/ismej.2014.178)

14. Chen C, Uematsu K, Linse K, Sigwart JD. 2017 By more ways than one: Rapid convergence at hydrothermal vents shown by 3D anatomical reconstruction of Gigantopelta (Mollusca: Neomphalina). *BMC Evolutionary Biology* **17**, 62. (doi:10.1186/s12862-017-0917-z)

15. Chen C, Pradillon F, Diaz-Recio Lorenzo C, Alfaro-Lucas JM. 2025 Integrative taxonomy of two new peltospirid gastropods from Mid-Atlantic Ridge hot vents, including a potentially symbiotic species. *Zoological Journal of the Linnean Society* **204**, zlaf055. (doi:10.1093/zoolinnean/zlaf055)

16. Methou P, Guéganton M, Copley JT, Kayama Watanabe H, Pradillon F, Cambon-Bonavita M-A, Chen C. 2024 Distinct development trajectories and symbiosis modes in vent shrimps. *Evolution* **78**, 413–422. (doi:10.1093/evolut/qpad217)

17. Zbinden M, Cambon-Bonavita M. 2020 Biology and ecology of Rimicaris exoculata, a symbiotic shrimp from deep-sea hydrothermal vents. *Marine Ecology Progress Series* **652**, 187–222. (doi:10.3354/meps13467)

18. Cambon-Bonavita M-A, Aubé J, Cueff-Gauchard V, Reveillaud J. 2021 Niche partitioning in the Rimicaris exoculata holobiont: the case of the first symbiotic Zetaproteobacteria. *Microbiome* **9**, 1–16. (doi:10.1186/s40168-021-01045-6)

19. Methou P, Hikosaka M, Chen C, Watanabe HK, Miyamoto N, Makita H, Takahashi Y, Jenkins RG. 2022 Symbiont Community Composition in Rimicaris kairei Shrimps from Indian Ocean Vents with Notes on Mineralogy. *Applied and Environmental Microbiology* **88**, 1–16. (doi:10.1128/aem.00185-22)

20. Streit K, Bennett SA, Van Dover CL, Coleman M. 2015 Sources of organic carbon for Rimicaris hybisae: Tracing individual fatty acids at two hydrothermal vent fields in the Mid-Cayman rise. *Deep-Sea Research Part I: Oceanographic Research Papers* **100**, 13–20. (doi:10.1016/j.dsr.2015.02.003)

21. Methou P, Michel LN, Segonzac M, Cambon-Bonavita M-A, Pradillon F. 2020 Integrative taxonomy revisits the ontogeny and trophic niches of Rimicaris vent shrimps. *Royal Society Open Science* **7**, 200837. (doi:10.1098/rsos.200837)

22. Ponsard J *et al.* 2013 Inorganic carbon fixation by chemosynthetic ectosymbionts and nutritional transfers to the hydrothermal vent host-shrimp Rimicaris exoculata. *ISME journal* **7**, 96–109. (doi:10.1038/ismej.2012.87)

23. Nye V, Copley JTP, Tyler PA. 2013 Spatial Variation in the Population Structure and Reproductive Biology of Rimicaris hybisae (Caridea: Alvinocarididae) at Hydrothermal Vents on the Mid-Cayman Spreading Centre. *PLoS ONE* **8**. (doi:10.1371/journal.pone.0060319)

24. Methou P, Hernández-Ávila I, Cathalot C, Cambon-Bonavita M-A, Pradillon F. 2022 Population structure and environmental niches of Rimicaris shrimps from the Mid-Atlantic Ridge. *Marine Ecology Progress Series* **684**, 1–20. (doi:10.3354/meps13986)

25. Methou P, Cueff-Gauchard V, Michel LN, Gayet N, Pradillon F, Cambon-Bonavita M. 2023 Symbioses of alvinocaridid shrimps from the South West Pacific: No chemosymbiotic diets but conserved gut microbiomes. *Environmental Microbiology Reports* **15**, 616–630. (doi:10.1111/1758-2229.13201)

26. Gebruk AV, Southward EC, Kennedy H, Southward AJ. 2000 Food sources, behaviour, and distribution of hydrothermal vent shrimps at the Mid-Atlantic Ridge. *Journal of the Marine Biological Association of the United Kingdom* **80**, 485–499. (doi:10.1017/S0025315400002186)

27. Stevens CJ, Limén H, Pond DW, Gélinas Y, Juniper SK. 2008 Ontogenetic shifts in the trophic ecology of two alvinocaridid shrimp species at hydrothermal vents on the Mariana Arc, western Pacific Ocean. *Marine Ecology Progress Series* **356**, 225–237. (doi:10.3354/meps07270)

28. Methou P, Nye V, Copley JT, Watanabe HK, Nagai Y, Chen C. 2023 Life history traits of alvinocaridid shrimps inhabiting chemosynthetic ecosystems around Japan. *Marine Biology* **170**, 1–17. (doi:10.1007/s00227-023-04221-4)

29. Apremont V, Cambon-Bonavita M-A, Cueff-Gauchard V, François D, Pradillon F, Corbari L, Zbinden M. 2018 Gill chamber and gut microbial communities of the hydrothermal shrimp Rimicaris chacei Williams and Rona 1986: A possible symbiosis. *PLoS ONE* **13**, e0206084. (doi:10.1371/journal.pone.0206084)

30. Coplen TB. 2011 Guidelines and recommended terms for expression of stable-isotope-ratio and gas-ratio measurement results. *Rapid Communications in Mass Spectrometry* **25**, 2538–2560. (doi:10.1002/rcm.5129)

31. Mathieu-Resuge M, Le Grand F, Brosset P, Lebigre C, Soudant P, Vagner M, Pecquerie L, Sardenne F. 2023 Red muscle of small pelagic fishes' fillets are high-quality sources of essential fatty acids. *Journal of Food Composition and Analysis* **120**, 105304. (doi:10.1016/j.jfca.2023.105304)

32. R Core Team . 2021 R: A language and environment for statistical computing. See https://www.r-project.org.

33. Aznar-Cormano L, Brisset J, Chan TY, Corbari L, Puillandre N, Utge J, Zbinden M, Zuccon D, Samadi S. 2015 An improved taxonomic sampling is a necessary but not sufficient condition for resolving inter-families relationships in Caridean decapods. *Genetica* **143**, 195–205. (doi:10.1007/s10709-014-9807-0)

34. Ronquist F, Teslenko M, Van Der Mark P, Ayres DL, Darling A, Höhna S, Liu L, Suchard MA, Huelsenbeck JP. 2012 MrBayes 3.2: Efficient Bayesian Phylogenetic Inference and Model Choice Across a Large Model Space. *Systematic Biology* **61**, 539–542. (doi:10.1093/sysbio/sys029)

35. Darriba D, Posada D, Kozlov AM, Stamatakis A, Morel B, Flouri T. 2020 ModelTest-NG: A New and Scalable Tool for the Selection of DNA and Protein Evolutionary Models. *Molecular Biology and Evolution* **37**, 291–294. (doi:10.1093/molbev/msz189)

36. Revell LJ. 2011 phytools: an R package for phylogenetic comparative biology (and other things). *Methods in Ecology and Evolution*

37. Pond DW, Dixon DR, Bell MV, Fallick AE, Sargent JR, David W, Sargentl JR. 1997 Occurrence of 16:2(n-4) and 18:2(n-4) fatty acids in the lipids of the hydrothermal vent shrimps Rimicaris exoculata and Alvinocaris markensis: nutritional nutritional and trophic implications. *Marine Ecology Progress Series* **156**, 167–174. (doi:10.3354/meps156167)

38. Russell NJ, Nichols DS. 1999 Polyunsaturated fatty acids in marine bacteria — a dogma rewritten. *Microbiology* **145**, 767–779. (doi:10.1099/13500872-145-4-767)

39. Nichols DS. 2003 Prokaryotes and the input of polyunsaturated fatty acids to the marine food web. *FEMS Microbiology Letters* **219**, 1–7. (doi:10.1016/S0378-1097(02)01200-4)

40. McCaffrey MA, Farrington JW, Repeta DJ. 1989 Geochemical implications of the lipid composition of Thioploca spp. from the Peru upwelling region—15°S. *Organic Geochemistry* **14**, 61–68. (doi:10.1016/0146-6380(89)90019-3)

41. Schoener TW. 1974 Resouce partitioning in ecological communities: Research on how similar species divide resources helps. *Science* **185**, 27–39.

42. Beinart RA *et al.* 2012 Evidence for the role of endosymbionts in regional-scale habitat partitioning by hydrothermal vent symbioses. *Proceedings of the National Academy of Sciences* , 241–250. (doi:10.1073/pnas.1202690109)

43. Riou V *et al.* 2010 Mixotrophy in the deep sea: A dual endosymbiotic hydrothermal mytilid assimilates dissolved and particulate organic matter. *Marine Ecology Progress Series* **405**, 187–201. (doi:10.3354/meps08515)

44. Demopoulos AWJ, McClain-Counts JP, Bourque JR, Prouty NG, Smith BJ, Brooke S, Ross SW, Ruppel CD. 2019 Examination of Bathymodiolus childressi nutritional sources, isotopic niches, and food-web linkages at two seeps in the US Atlantic margin using stable isotope analysis and mixing models. *Deep Sea Research Part I: Oceanographic Research Papers* **148**, 53–66. (doi:10.1016/j.dsr.2019.04.002)

45. Yang Y, Sun J, Chen C, Zhou Y, Van Dover CL, Wang C, Qiu J-W, Qian P-Y. 2022 Metagenomic and metatranscriptomic analyses reveal minor-yet-crucial roles of gut microbiome in deep-sea hydrothermal vent snail. *Animal Microbiome* **4**. (doi:10.1186/s42523-021-00150-z)

46. Methou P, Johnson SB, Sherrin J, Shank TM, Chen C, Tunnicliffe V. 2024 A tale of two shrimps – Speciation and demography of two sympatric shrimp species from hydrothermal vents. , 2024.12.18.629080. (doi:10.1101/2024.12.18.629080)

47. Gao K *et al.* 2025 Phylogenomic analyses of Pliocardiinae (Bivalvia: Vesicomyidae) update genus-level taxonomy and shed light on trait evolution. *Cladistics* , cla.70001. (doi:10.1111/cla.70001)

48. Breusing C, Johnson SB, Tunnicliffe V, Clague DA, Vrijenhoek RC, Beinart RA. 2020 Allopatric and sympatric drivers of speciation in alviniconcha hydrothermal vent snails. *Molecular Biology and Evolution* **37**, 3469–3484. (doi:10.1093/molbev/msaa177)

49. Li Y, Kocot KM, Whelan NV, Santos SR, Waits DS, Thornhill DJ, Halanych KM. 2017 Phylogenomics of tubeworms (Siboglinidae, Annelida) and comparative performance of different reconstruction methods. *Zoologica Scripta* **46**, 200–213. (doi:10.1111/zsc.12201)

50. Joey Pakes M, Mejía-Ortiz L, Weis AK. 2014 Arthropods host intracellular chemosynthetic symbionts, too: cave study reveals an unusual form of symbiosis. *Journal of Crustacean Biology* **34**, 334–341. (doi:10.1163/1937240X-00002238)

51. Hammer TJ, Moran NA. 2019 Links between metamorphosis and symbiosis in holometabolous insects. *Philosophical Transactions of the Royal Society B: Biological Sciences* **374**, 20190068. (doi:10.1098/rstb.2019.0068)

52. Corbari L, Zbinden M, Cambon-Bonavita MA, Gaill F, Compère P. 2008 Bacterial symbionts and mineral deposits in the branchial chamber of the hydrothermal vent shrimp rimicaris exoculata: Relationship to moult cycle. *Aquatic Biology* **1**, 225–238. (doi:10.3354/ab00024)

53. Alfaro-Lucas JM, Chapman ASA, Tunnicliffe V, Bates AE. 2024 High functional vulnerability across the world's deep-sea hydrothermal vent communities. *Proc. Natl. Acad. Sci. U.S.A.* **121**, e2403899121. (doi:10.1073/pnas.2403899121)

54. Zhang H, Yahagi T, Miyamoto N, Chen C, Jiang Q, Qian P-Y, Sun J. 2025 Circatidal control of gene expression in the deep-sea hot vent shrimp *Rimicaris leurokolos*. *Proc. R. Soc. B.* **292**, 20242970. (doi:10.1098/rspb.2024.2970)

55. Tandberg AH, Rapp HT, Schander C, Vader W, Sweetman AK, Berge J. 2012 Exitomelita sigynae gen. et sp. nov.: A new amphipod from the Arctic Loki Castle vent field with potential gill ectosymbionts. *Polar Biology* **35**, 705–716. (doi:10.1007/s00300-011-1115-x)

56. Zbinden M, Marqué L, Gaudron SM, Ravaux J, Léger N, Duperron S. 2015 Epsilonproteobacteria as gill epibionts of the hydrothermal vent gastropod Cyathermia naticoides (North East-Pacific Rise). *Marine Biology* **162**, 435–448. (doi:10.1007/s00227-014-2591-7)